J|A|C|S ARTICLES

Published on Web 05/07/2009

Carbon Dioxide and Methane Transport in DDR Zeolite: Insights from Molecular Simulations into Carbon Dioxide Separations in Small Pore Zeolites

Sang Eun Jee and David S. Sholl*

School of Chemical and Biomolecular Engineering, Georgia Institute of Technology, 311 Ferst Drive, Atlanta, Georgia 30332-0100

Received February 25, 2009; E-mail: david.sholl@chbe.gatech.edu

Abstract: The silica zeolite DDR is a strong candidate for separations of CO_2/CH_4 because of the narrow windows that control molecular transport inside the material's pores. We have used molecular simulations to describe diffusion of CO_2 and CH_4 inside DDR pores. Our simulations introduce a new force-field for this system that for the first time gives results that are consistent with experimental measurements of single-component adsorption and diffusion. Diffusivities obtained from previous simulations greatly overestimated the transport rates of CH_4 and, to a lesser extent, CO_2. Because CH_4 diffuses extremely slowly in DDR, we applied a transition state theory-based kinetic Monte Carlo scheme to accurately describe this diffusion. The most important observation from our calculations is that the characteristics of CO_2/CH_4 diffusion in DDR are very different from the usual situation in nanoporous materials, where the presence of a slowly diffusing species retards transport rates of a more rapidly diffusing species. In DDR, we show that CO_2 diffusion rates are only weakly affected by the presence of CH_4, despite the very slow diffusion of the latter molecules. The physical origins of this unusual behavior are explained by analyzing the adsorption sites and diffusion mechanism for each species. Our finding suggests DDR membranes are favorable for CO_2/CH_4 separations and that similar properties may exist for other 8MR zeolites.

1. Introduction

Separation of CO_2 from CH_4 is an important problem because of the large volumes of natural gas that are known to contain high levels of CO_2.[1,2] Development of robust materials to achieve this gas separation in an energy efficient manner would have a significant impact on the possibility of using these resources in a manner that mitigates CO_2 emissions. Using small pore zeolites as separation membranes is an attractive approach to this challenge. A number of studies have focused on membranes made from SAPO-34, an aluminophosphate material with 8-membered rings (8MR).[3,4] Several pure silica zeolites also have pores defined by 8MR. Among these, the silica zeolite DDR ($Si_{120}O_{240}$) is especially attractive. The 8MR windows are 0.36×0.44 nm in size, similar in size to CH_4 but larger than CO_2.[5] This, in addition to the hydrophilic character of DDR, has led several groups to consider the use of DDR as a membrane for CO_2-related gas separations.[6−11]

Despite the work that has been reported with DDR membranes, some important issues remain unresolved. To design a process using a zeolite membrane, it is essential to understand how mixtures of the relevant species adsorb and diffuse through the zeolite. Characterizing mixture diffusion in zeolites via experiments is a challenging task, and molecular simulations have become an important tool in providing a detailed physical understanding of how diffusion in adsorbed mixtures occurs.[9,10,12−18] Molecular simulations have been reported to accurately describe the experimentally observed single-component adsorption of CH_4 and CO_2 in DDR, and these simulations have highlighted features of the mixture adsorption of these species that are quite unusual as compared to other zeolites and nanoporous materials.[9,10] As we will show below, the force-fields that were used in this previous work give inaccurate predictions of single-

(1) Baker, R. W. *Membrane Technology and Applications*; McGraw-Hill: New York, 2000.
(2) Baker, R. W. *Ind. Eng. Chem. Res.* **2002**, *41*, 1393–1411.
(3) Li, S. G.; Falconer, J. L.; Noble, R. D. *J. Membr. Sci.* **2004**, *241*, 121–135.
(4) Li, S. G.; Falconer, J. L.; Noble, R. D. *Adv. Mater.* **2006**, *18*, 2601–2603.
(5) Gies, H. *Z. Kristallogr.* **1986**, *175*, 93–104.
(6) Zhu, W.; Kapteijn, F.; Moulijn, J. A.; den Exter, M. C. *Langmuir* **2000**, *16*, 3322–3329.
(7) Zhu, W.; Kapteijn, F.; Moulijn, J. A.; Jansen, J. C. *Phys. Chem. Chem. Phys.* **2000**, *8*, 1773–2779.
(8) Chen, H.; Sholl, D. S. *Langmuir* **2007**, *23*, 6431–6437.
(9) Krishna, R.; van Baten, J. M. *Chem. Phys. Lett.* **2007**, *446*, 344–349.
(10) Krishna, R.; van Baten, J. M. *Sep. Purif. Technol.* **2008**, *61*, 414–423.
(11) Tomita, T.; Nakayama, K.; Sakai, H. *Microporous Mesoporous Mater.* **2004**, *68*, 71–75.
(12) Sholl, D. S. *Acc. Chem. Res.* **2006**, *39*, 403–411.
(13) Skoulidas, A. I.; Sholl, D. S. *J. Phys. Chem. B* **2001**, *105*, 3151–3154.
(14) Skoulidas, A. I.; Sholl, D. S. *J. Phys. Chem. B* **2002**, *106*, 5058–5067.
(15) Krishna, R.; Paschek, D. *Phys. Chem. Chem. Phys.* **2002**, *4*, 1891–1898.
(16) Krishna, R.; van Baten, J. M. *Ind. Eng. Chem. Res.* **2006**, *45*, 2084–2093.
(17) Krishna, R.; van Baten, J. M.; Garcia-Perez, E.; Calero, S. *Chem. Phys. Lett.* **2006**, *429*, 219–224.
(18) Paschek, D.; Krishna, R. *Phys. Chem. Chem. Phys.* **2001**, *3*, 3185–3191.

10.1021/ja901483e CCC: $40.75

component diffusion rates when compared to experimental measurements.[9,10] This means that previous efforts to characterize molecular diffusion in DDR via molecular simulations cannot reliably describe the properties of diffusing mixtures.

In this Article, we describe a series of molecular simulations that provide the most accurate description of CO_2/CH_4 mixture transport in DDR to date. Throughout this article, we consider this adsorbed mixture at room temperature. The implications of our results for other temperatures are discussed in section 7. Our results highlight some unusual properties of this material that greatly enhance its ability as a membrane for this gas separation. These calculations required a novel combination of simulation methods that will also be useful in studies of other small pore zeolites. We first introduce a new force-field that, for the first time, correctly describes the diffusion coefficients for single-component CO_2 and CH_4 at low loading that have been reported experimentally. In developing this force-field, we focused on the characteristics of the transition states that control molecular hopping between adsorption sites in DDR. Previous force-fields have been based only on adsorption data,[19] meaning that they probe the energetic environment near preferred adsorption sites but include almost no information about transition states for diffusion. The experimentally observed diffusivities for CH_4 in DDR point to a complication that has not been addressed in previous treatments of this system, that this molecule diffuses so slowly that its diffusion cannot be successfully described using Molecular Dynamics (MD) simulations. To address this issue, we used a transition state theory (TST) approach to characterize the site-to-site hopping rates of CH_4 as a function of molecular loading in DDR. Subsequent kinetic Monte Carlo (KMC) simulations using our TST-derived hopping rates provide information on the loading-dependent diffusivity of CH_4. CO_2 diffuses much more rapidly than CH_4, so it is possible to assess this diffusion using standard MD methods.

The combination of rapidly diffusing CO_2 and slowly diffusing CH_4 in DDR superficially makes this material extremely attractive for membrane-based separations, because this difference in diffusivities can enhance the adsorption-based selectivity of DDR for CO_2 relative to CH_4. Unfortunately, a general expectation for mixture diffusion in nanoporous materials is that the presence of a slower species will retard the diffusion of a more mobile species, and vice versa.[12,15,18,20] When this occurs, any beneficial effects that might be inferred from differences in single-component diffusivities tend to be diminished under practical conditions where transport of an adsorbed mixture occurs. We show via molecular simulations that this outcome does not occur for CO_2/CH_4 mixtures in DDR. Instead, for adsorbed mixtures with compositions relevant for practical applications, the diffusive transport of CO_2 is only weakly affected by the presence of CH_4, while the slowly diffusing CH_4 molecules are retarded by the more rapidly diffusing CO_2 molecules. This is a very unusual situation with important implications for using this material in membrane-based applications. We show that this phenomenon can be understood in terms of the diffusion mechanisms of each species. This understanding should make it possible to identify other small pore materials that would also exhibit this favorable property.

(19) Dubbeldam, D.; Calero, S.; Vlugt, T. J. H.; Krishna, R.; Massen, T. L. M.; Smit, B. *J. Phys. Chem. B* **2004**, *108*, 12301–12313.
(20) Maceiras, D. B.; Sholl, D. S. *Langmuir* **2002**, *18*, 7393–7400.

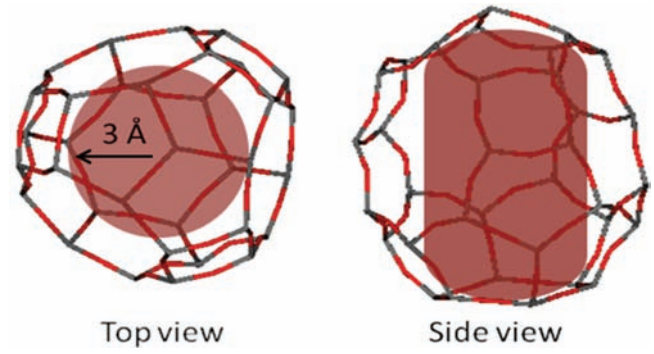

Figure 1. Top and side views of a single 19-hedra cage in DDR, with shaded regions indicating the cylindrical volume with radius 3 Å associated with adsorption in this cage. In the top view, the three 8MR are visible to the right, the bottom left, and top left.

Table 1. Interaction Potential and Force-Field Parameters of CH_4, CO_2 in DDR Structures Are Developed To Reproduce Experimental Data

CH_4-CH_4	CH_4-O_{zeo}	$C_{CO2}-C_{CO2}$	$O_{CO2}-O_{CO2}$	$O_{zeo}-O_{zeo}$
$n = 12$	$n = 18$	$n = 12$	$n = 12$	$n = 18$
$C_1 = 4$	$C_1 = 4$	$C_1 = 4$	$C_1 = 4$	$C_1 = 4$
$C_2 = 4$	$C_2 = 3$	$C_2 = 4$	$C_2 = 4$	$C_2 = 3$
$\varepsilon/k_B =$ 147.9 [K]	$\varepsilon/k_B =$ 160.9 [K]	$\varepsilon/k_B =$ 28.129 [K]	$\varepsilon/k_B =$ 80.507 [K]	$\varepsilon/k_B =$ 76 [K]
$\sigma = 3.73$ [Å]	$\sigma = 3.218$ [Å]	$\sigma = 2.757$ [Å]	$\sigma = 3.033$ [Å]	$\sigma = 2.5$ [Å]

The difference in time scales between CH_4 diffusion and CO_2 diffusion in DDR raises technical challenges for accurately describing mixture diffusion with molecular simulations. We show that these challenges can be overcome by a judicious combination of MD and TST-based KMC simulations. The methods we introduce for this purpose should be useful in the future for other materials in which separations based on large differences in diffusion rates are considered.

2. Methods

We used the DDR crystal structure measured experimentally by Gies et al.[5] The 19-hedra cages in DDR are the only cages relevant for molecular transport; the decahedral and dodecahedral cages are not accessible to diffusing molecules. Molecules were not allowed to adsorb inside the smaller cages in our simulations. The structure of one of the 19-hedra cages that defines the accessible volume in DDR is shown in Figure 1.

Our simulations treated the DDR crystal as being rigid. The molecule−DDR interaction energies were precomputed for a high-resolution spatial grid, and in subsequent simulations these energies were computed by high-quality interpolation from the precomputed values. Periodic boundary conditions were used in all simulations. All calculations were performed at room temperature.

CH_4-CH_4 and CO_2-CO_2 interactions were treated using the potentials introduced by Goodbody et al.[21] and Makrodimitris et al.[22] without adjustment. The potentials are summarized in Table 1. All cross-species interactions were defined using Lorenz−Berthelot combining rules based on the interaction potentials listed in Table 1. All calculations used spherical cutoffs of radius 13 Å for Lennard-Jones potentials and 25 Å for the Coulombic contributions to CO_2-CO_2 interactions.

Grand canonical Monte Carlo (GCMC) was used to calculate adsorption isotherms in a simulation volume containing 6 DDR

(21) Goodbody, S. J.; Watanabe, K.; MacGowan, D.; Walton, J. P. R. B.; Quirke, N. *J. Chem. Soc., Faraday Trans.* **1991**, *87*, 1951–1958.
(22) Makrodimitris, K.; Papadopoulos, G. K.; Theodorou, D. N. *J. Phys. Chem.* **2001**, *105*, 777–788.

unit cells. These simulations involved a total of 5×10^7 moves for equilibration and up to 5×10^7 moves for data collection for each state point. All results below are reported in terms of fugacities. At the highest fugacities we simulated, the nonideality of CO_2 would need to be included to convert fugacities to pressures.

As we will show below, single-component diffusion of CH_4 in DDR gives diffusivities less than 10^{-7} cm^2/s in most cases, making simulation of this situation with MD challenging. We only applied MD to measure single-component diffusion in cases where the resulting diffusivity was larger than 10^{-7} cm^2/s. This restriction allowed us to examine CO_2 diffusion at all loadings with MD, but only a small number of CH_4 loadings. MD simulations were performed using a simulation volume of 6−24 unit cells, depending on the adsorbate loading. In single-component MD simulations, $(2 \times 10^7)-(4 \times 10^7)$ GCMC steps were used to initialize each system with the desired number of molecules. We found that this procedure was important to correctly distribute molecules on DDR's inhomogeneous potential energy surface. Each simulation was further equilibrated with 1.5×10^7 canonical MC moves and 1.5×10^7 MD steps. Data were then collected from MD simulations 20 ns in duration using 1 fs time-steps. These MD simulations were used to measure both the self-diffusivity, D_s, and the corrected diffusivity, D_0, by averaging over 30 independent trajectories for each adsorbate loading.[12,14,23]

As mentioned above, MD is not suitable for accurately simulating CH_4 diffusion in DDR because of its slow diffusion. Instead, we developed a transition state theory (TST)-based lattice model that accurately describes the loading-dependent diffusion of CH_4 in DDR. Once this model is defined, kinetic Monte Carlo (KMC) can be used to simulate diffusion. This approach is based on the methods of Tunca and Ford[24−27] and the subsequent work by Dubbledam and co-workers.[28,29] We define the hopping rate of CH_4 molecules from a DDR cage containing i molecules into an adjacent cage containing j molecules as

$$k_{ij} = \kappa \sqrt{\frac{1}{2\beta\pi m}} \frac{\exp(-\beta F(q^*))}{\int \mathrm{d}q \exp(-\beta F(q))} \qquad (1)$$

where $\beta = (k_B T)^{-1}$, q is the reaction coordinate, q^* defines the dividing plane associated with the transition state, $F(q)$ is the system's free energy when the moving molecule is at q, and the integral is evaluated over the microstate defined by one DDR cage. We assume that the transmission coefficient, κ, is unity. At some loadings, it is possible to directly compare MD simulations with our TST/KMC results, and we show below that these two methods are in good agreement, supporting the validity of this treatment. We find that the maximum loading of CH_4 in DDR is 5 molecules per cage, so 6×5 distinct hopping rates, k_{ij}, were computed with $1 \le i \le 5$ and $0 \le j \le 5$. Once these rates are known, KMC can be used to simulate net diffusion at any loading of interest.

To apply eq 1, we computed the free energy, $F(q)$, using a histogram sampling method.[25,26] We considered a dividing surface in the middle of an 8MR window as q^*. At the beginning of the simulation, molecules are inserted in each site at the loadings required for the transition rate of interest. 1×10^8 canonical MC moves per particle were then used to equilibrate system, and 2×10^8 canonical moves were used to produce data. All degrees of freedom, that is, the positions of all adsorbed molecules at the loading of interest, were sampled in these simulations. Moves that would have transferred molecules past the dividing surface were rejected. After every MC step, particle positions are recorded, allowing the free energy to be computed using $F\beta(q) = -\ln\langle P(q)\rangle$, where $P(q)$ is the probability that the molecule of interest lies at reaction coordinate q. No bias potential was applied during these calculations.

3. Force-Fields for Single-Component Adsorption and Diffusion

Previous simulations of CH_4 and CO_2 adsorption in DDR[9,10] were based on adsorbate−zeolite potentials introduced by Dubbeldam et al.[19] and Makrodimitris et al.[22] However, we have found these potentials do not reproduce recently reported experimental data by Hedin et al. and Chance et al.[30,31] Figure 2a shows adsorption isotherms from GCMC simulations for CO_2 and CH_4 in DDR at 298 K using the force-fields cited above, as well as experimental data.[30,31] The uncertainties in the simulated data are smaller than the symbol sizes. Our adsorption isotherms are presented in terms of molecules per unit cell and fugacity. A loading of 1 molecule/unit cell corresponds to 2.22 (6.11) mg/g adsorption for CH_4 (CO_2). To allow a comparison with experimental data, the Peng−Robinson equation of state was used to estimate the fugacity associated with the experimentally reported pressures. It is clear from Figure 2a that these interatomic potentials provide a reasonable description of CO_2 and CH_4 adsorption in DDR.

Figure 2b shows the computed self-diffusion coefficients for CO_2 and CH_4 from simulations using the interatomic potentials defined above. These results for both species were computed using MD because the predicted diffusion coefficients are larger than 10^{-7} cm^2/s. These results are compared to experimental data for diffusion of each species at dilute loadings, which is also shown in the same figure.[30,31] In contrast to the adsorption isotherms, the predicted diffusion coefficients differ strongly from the experimental data. These simulations overpredict the CH_4 (CO_2) diffusivity at dilute loadings by about 2 orders (1 order) of magnitude. It is useful to note that because the diffusion data in Figure 2b come from PFG-NMR experiments, it is clear that the slow diffusion that is observed is associated with the intrinsic pore topology of DDR, not with intracrystalline grain boundaries or other defects that might affect diffusion rates over large length scales.

Motivated by this observation, we have developed new force-fields that are more consistent with the experimental adsorption and diffusion data. To improve the treatment of diffusion for each species, we focused on the transition states for diffusion of each molecule. In DDR, CH_4 adsorbs inside the zeolite cages,[9,10] and the transition states for CH_4 diffusion are the 8MR rings that separate adjacent cages. The energy of CH_4 in the 8MR is strongly influenced by the repulsive core of the CH_4−O potential. We examined CH_4−O potentials of the form

$$V(r) = \varepsilon\left(\frac{C_1}{(r/\sigma)^n} - \frac{C_2}{(r/\sigma)^6}\right) \qquad (2)$$

When $n = 12$ and $C_1 = C_2 = 4$, this is the standard LJ potential. For other values of n, we defined C_1 and C_2 so the minimum of the resulting potential lies at the same coordinate as the standard LJ potential and so that they have minimal differences in energy at the coordinates that define the inflection points of the two potentials. With these choices, the differences in adsorption energy between the two potentials are small in the vicinity of the energy minima that dominate adsorption. After examining a range of parameters, we found that the slow diffusion of CH_4 observed experimentally could best be reproduced by using $n = 18$ instead of 12. The key feature of this approach is that the

(23) Maginn, E. J.; Bell, A. T.; Theodorou, D. N. *J. Phys. Chem.* **1993**, *97*, 4173–4181.
(24) Ford, D. M.; Glandt, E. D. *J. Phys. Chem.* **1995**, *99*, 11543–11549.
(25) Tunca, C.; Ford, D. M. *Chem. Eng. Sci.* **2003**, *58*, 3373–3383.
(26) Tunca, C.; Ford, D. M. *J. Chem. Phys.* **2004**, *120*, 10763–10767.
(27) Tunca, C.; Ford, D. M. *J. Chem. Phys.* **1999**, *111*, 2751–2760.

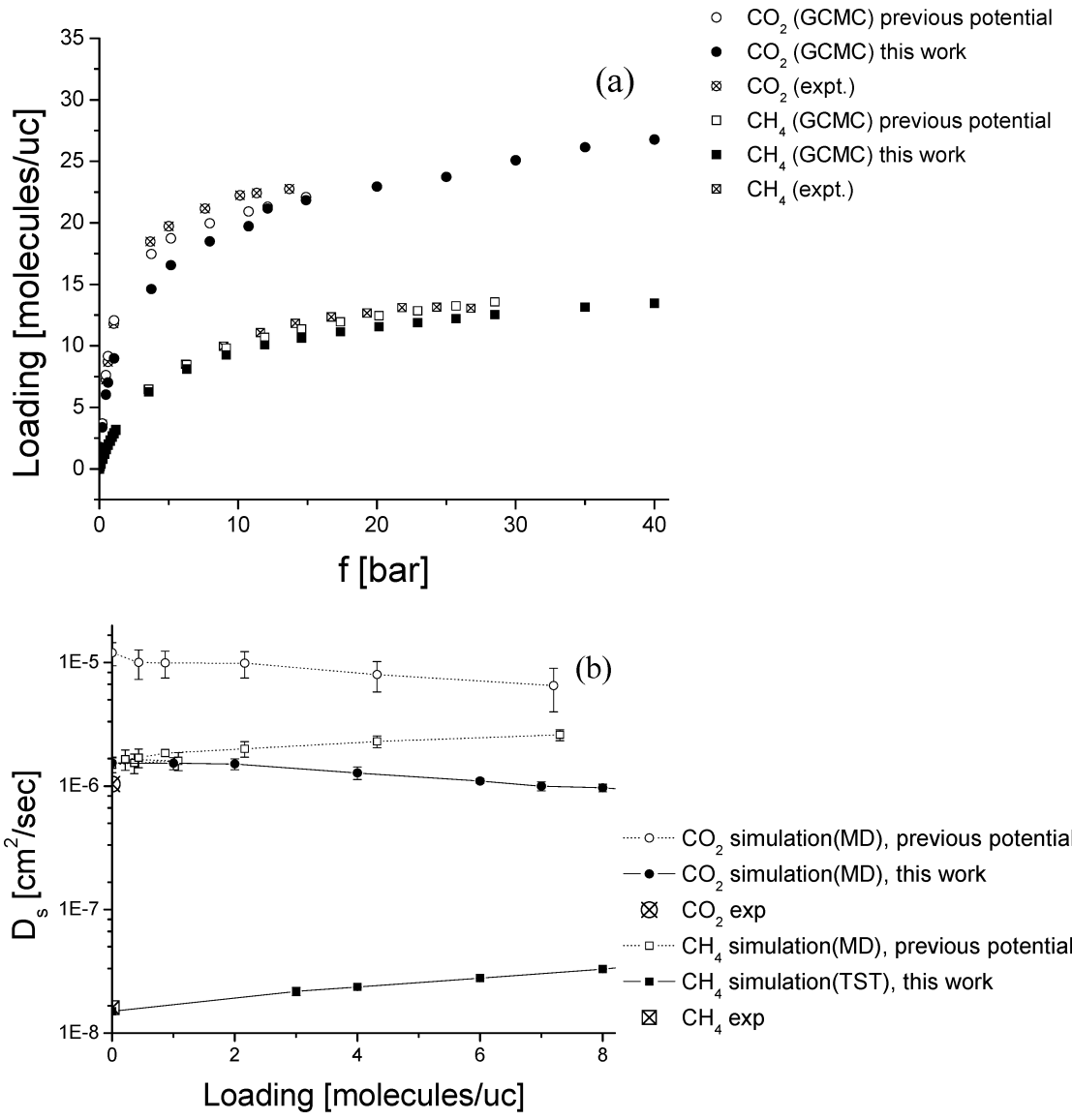

Figure 2. (a) Single-component adsorption isotherms of CO_2 and CH_4 in DDR from GCMC simulations and experiments at 298 K. Open symbols show GCMC simulation results using a previous potential;[19] closed symbols show GCMC results using potentials from this work. Crossed symbols show experimental data.[30,31] (b) Single-component self-diffusivities of CO_2 and CH_4 in DDR from MD simulations at 298 K, using the same notation as (a).

repulsive wall of the potential is considerably steeper than the standard Lennard-Jones potential. It was not possible to correctly describe CH_4 diffusion and adsorption using potentials that varied the well depth of the potential without also varying the steepness of the repulsive portion of the potential.

The adsorption sites of CO_2 in DDR are very different from CH_4. The most energetically preferred sites for CO_2 adsorption lie inside the 8MR, with CO_2 adsorbing in the zeolite's cages only after the 8MR are occupied.[9,10] Diffusion of CO_2 in DDR is controlled by the transition state for hopping of CO_2 from an 8MR into an adjacent cage. Examination of this TS indicated that the TS energy is primarily controlled by the electrostatic interactions between CO_2 and the zeolite. As a result, the only avenue for significantly altering the energy of this TS while retaining the form of the interatomic potentials defined above was to increase the partial charges of O and Si. We chose to increase these charges to $-1.5e$ and $+3e$, which are considerably larger than would typically be assigned in materials of this kind.[22,32−34] Using smaller charges significantly decreased the agreement between the diffusivities calculated with MD and the experimental data. Because increasing these charges increases adsorption of CO_2 in DDR, the LJ parameters for interactions between atoms in CO_2 and the framework oxygens were also adjusted. An 18−6 LJ potential was used for these interactions because we found that this slightly increased the TS energy relative to the energy minimum in the 8MR. The effect of modifying the LJ potential in this way was relatively small as compared to the effect of the framework partial charges. By making these adjustments, our force-field simultaneously reproduces the Henry's coefficient of adsorption and the dilute loading diffusivity at the same time.

Table 1 summarizes our new force-field. With our potential, we calculated adsorption with GCMC and diffusion using MD (for CO_2) and TST-based KMC (for CH_4), giving the results shown in Figure 2. By construction, these potentials reproduce the experimental adsorption isotherms and dilute loading diffusivities with reasonable (although not perfect) accuracy. We emphasize that this force-field was derived by treating the zeolite framework as rigid, as were earlier force-fields in the

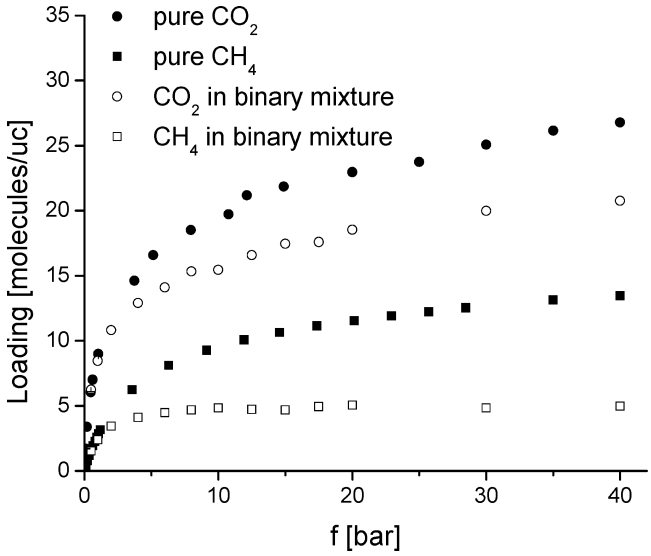

Figure 3. Single-component (filled symbols) and binary adsorption (open symbols) isotherms of CO_2 and CH_4 in DDR from GCMC simulations. The binary adsorption isotherm is for an equimolar bulk phase. Circles and rectangles represent CO_2 and CH_4.

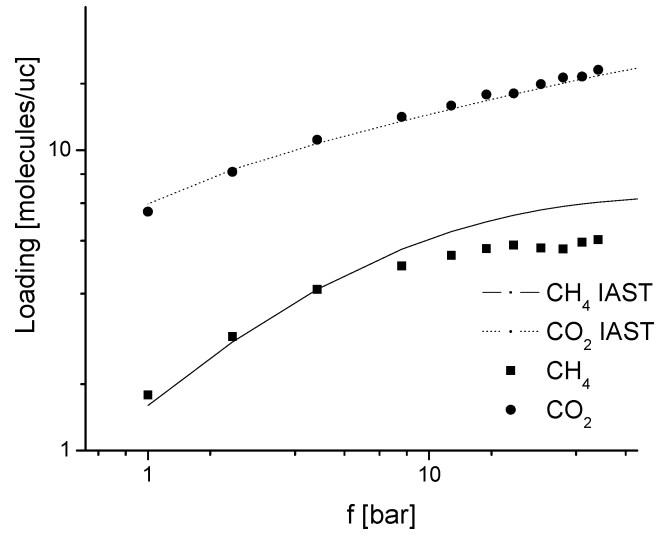

Figure 4. Binary adsorption isotherm data from GCMC (symbols) and modified IAST (curves) for adsorption from an equimolar bulk CO_2/CH_4 mixture.

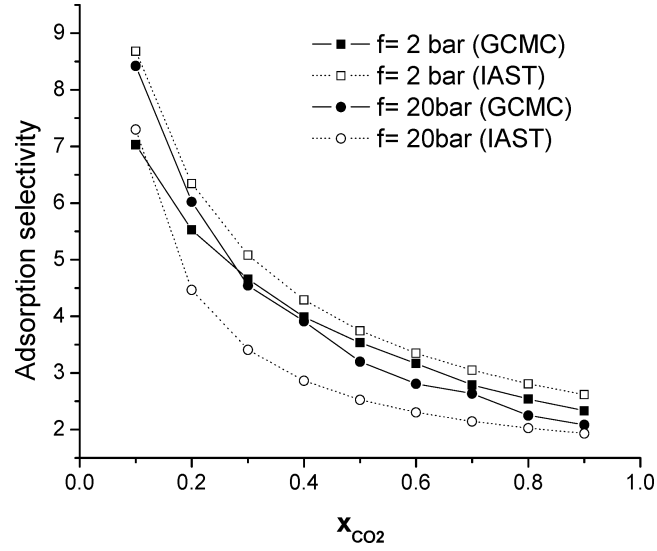

Figure 5. Adsorption selectivities from GCMC (filled symbols) and modified IAST (open symbols) are shown as a function of mole fraction of CO_2 in the bulk phase. Squares (circles) show results from a bulk phase fugacity of 2 (20) bar.

literature. If a flexible framework was to be considered, a new force-field for molecule−framework interactions would have to be developed for this approach to yield results consistent with the experimental data. The adsorption isotherms from the earlier potentials and our new potentials are similar, although the earlier CO_2 potential is in better agreement with the experimental isotherm over the full range of pressures for which data are available. In the remainder of this Article, we use the force-field introduced above to examine adsorption and diffusion of CO_2/CH_4 mixtures in DDR at 300 K.

4. Mixture Adsorption

As described above, CO_2 and CH_4 molecules prefer different adsorption sites in DDR.[9,10] Understanding the impact of these sites on adsorption of CO_2/CH_4 mixtures is important for understanding diffusion of these molecules, so in this section we highlight several aspects of CO_2/CH_4 adsorption. CO_2 adsorbs more strongly than CH_4 in single component as well as binary adsorption, as shown in Figures 3 and 4, which show GCMC results for adsorption from an equimolar gas phase mixture. Figure 5 shows GCMC results for mixture adsorption over a range of bulk compositions at two representative fugacities. The adsorption selectivities for CO_2 relative to CH_4 are 2−9 under these conditions.

To characterize where molecules adsorbed in DDR, we divided adsorption into volumes associated with 8MR windows and DDR cages for CO_2 and CH_4. The main cages of DDR are similar to spheres with radius 4 Å. We partitioned the pore volume by defining molecules with their center of mass located 3 Å or closer to the center of a cage as lying in a cage and all other molecules as being situated in a window. This partitioning differs slightly from the method used previously by Krishna,[9] but we feel it describes the geometry of the pore volume in a somewhat more natural way. Figure 6 shows a single-component adsorption isotherm in terms of the adsorbed amounts in the two regions. No CH_4 was found to adsorb in DDR's windows, so only total CH_4 loadings are shown in Figure 6. CO_2 prefers the windows at low total loadings and then occupies cages as the pressure is increased.[9,10] Figure 7 shows the adsorbed CO_2 molecules per window as a function of total adsorbed amount of CO_2 in both single-component and binary mixtures. It is clear that the CO_2 adsorption in DDR windows is almost independent of the CH_4 loading. This shows that CO_2 adsorption and CH_4 adsorption are competitive only in the cages.

The results above provide useful insight into predicting mixture adsorption isotherms in DDR using ideal adsorbed solution theory (IAST). IAST is a well-known method to predict mixture isotherms from single-component data,[35] but applying

(28) Dubbeldam, D.; Beerdsen, E. *J. Chem. Phys.* **2005**, *122*, 224712.
(29) Dubbeldam, D.; Calero, S.; Maesen, T. L. M.; Smit, B. *Phys. Rev. Lett.* **2003**, *90*, 245901.
(30) Chance, R. R. *229th ACS National Meeting*; San Diego, CA, Mar. 13−17, 2005.
(31) Hedin, N.; DeMartin, G. J.; Roth, W. J.; Strohmaier, K. G. *Microporous Mesoporous Mater.* **2008**, *109*, 327.
(32) Kramer, G. J.; Farragher, N. P.; van Beest, B. W. H.; van Santen, R. A. *Phys. Rev. B* **1991**, *43*, 5068–5080.

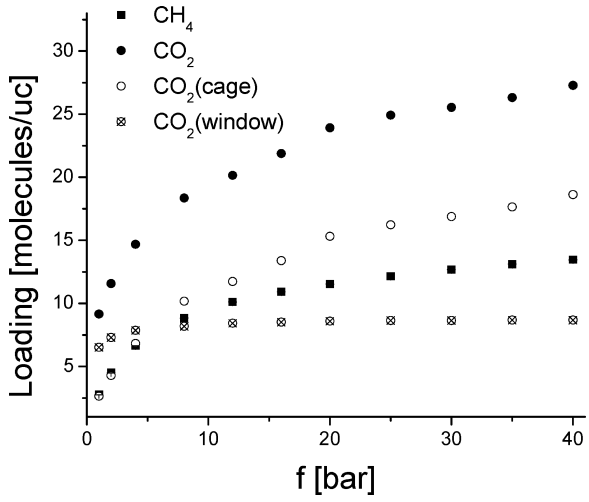

Figure 6. Single-component adsorption isotherms of CH_4 and CO_2 in DDR from GCMC with the contributions from the DDR cages and windows shown separately for CO_2.

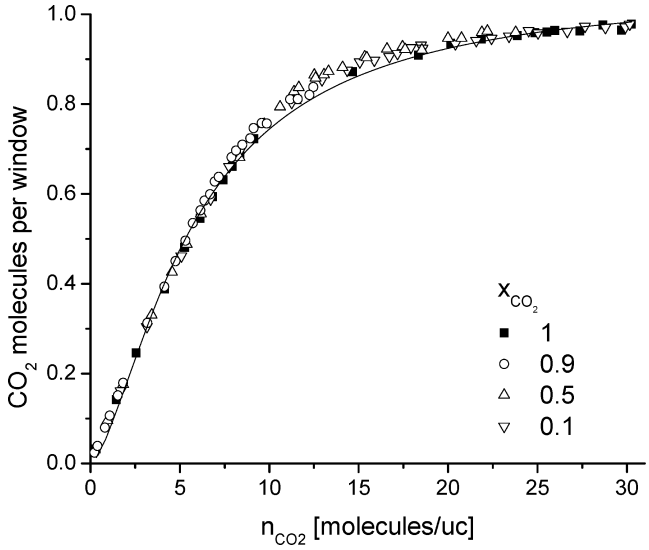

Figure 7. The number of CO_2 molecules per 8MR window as a function of total CO_2 loading in DDR for single-component adsorption (■) and mixture adsorption with CH_4 (open symbols) with the indicated bulk phase mole fractions. The solid line was fitted to the single-component data.

conventional IAST to CH_4/CO_2 mixtures in DDR overestimates (underestimates) the adsorbed amount of CO_2 (CH_4).[8−10] Figures 6 and 7 suggest that a simple modification of IAST can be used to describe mixture adsorption in this system. Specifically, we used IAST to describe the adsorption of mixtures of CH_4 and CO_2 in the cages of DDR, but then predicted the total adsorbed amount of CO_2 by adding the adsorbed CO_2 in the 8MR windows directly from our single-component data. Figure 4 shows that our modified IAST method works accurately for equimolar bulk mixtures, although the amount of CH_4 adsorption is overpredicted at the highest fugacities we examined. Figure 5 shows that this method also captures the trends in adsorption selectivity seen in our GCMC calculations as the composition of the bulk phase is varied. This application of IAST does not predict the mixture isotherms at high loadings with quantitative accuracy, but its performance is considerably better than the results of conventional IAST for this adsorbed mixture.[35]

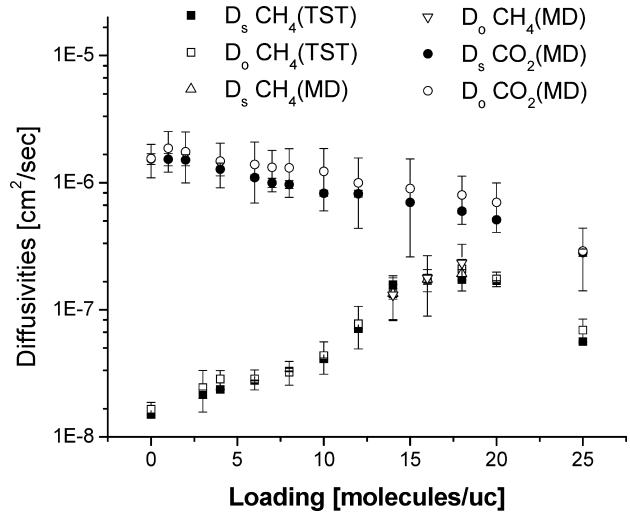

Figure 8. Calculated single-component diffusivities of CH_4 and CO_2 in DDR. All CO_2 results are from MD simulations. CH_4 results are shown at all loadings from TST-based KMC simulations and over a limited range of loadings from MD simulations.

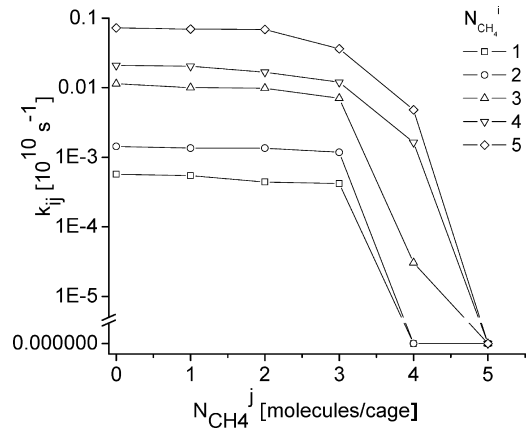

Figure 9. Hopping rate k_{ij} from i cage to j cage as calculated from TST shown as the number of the CH_4 molecules in the target cage, $N_{CH4}{}^j$. $N_{CH4}{}^i$ is the number of the CH_4 molecules in the cage from which the hopping CH_4 molecule departs.

5. Single-Component Diffusion of CO_2 and CH_4

Figure 8 shows single-component self-and corrected diffusivities, D_s and D_0, respectively, as a function of loading for CO_2 and CH_4 in DDR at 298 K from calculations using the new force-fields we described above. Here, the CO_2 results were computed using MD, while the CH_4 results were computed using TST-based KMC. The individual hopping rates determined from TST for CH_4 are shown in Figure 9. From Figure 8, three observations can be made. First, CO_2 diffuses 1−2 orders of magnitude faster than CH_4 in DDR at all loadings. This is an important observation for practical use of DDR as a membrane to separate CO_2/CH_4 mixtures, because it means that both adsorption and diffusion in this material favor transport of CO_2. Second, $D_0 \approx D_s$ for both species. That is, collective motions of the diffusing molecules are minimal,[14] a

(33) van Beest, B. W. H.; Kramer, G. J.; van Santen, R. A. *Phys. Rev. Lett.* **1990**, *64*, 1955–1958.
(34) Skoulidas, A. I.; Sholl, D. S.; Johnson, J. K. *J. Chem. Phys.* **2006**, *124*, 054708.
(35) Myers, A. L.; Prausnitz, J. M. *AIChE J.* **1965**, *11*, 121–127.

situation that is not unusual in cage-type zeolites.[28,29,36,37] Finally, the CO_2 diffusion coefficients decrease as a function of loading, while CH_4 diffusion initially increases as a function of loading and then decreases.

The qualitative trends in the loading-dependent diffusion coefficients of CH_4 and CO_2 can be understood in terms of the adsorption sites preferred by each species. For CH_4, diffusion is dominated by the large energy barrier that exists for molecules hopping through the 8MR windows between cages. As the CH_4 loading increases, adsorbate−adsorbate interactions between additional CH_4 molecules in the initial and final cages in this process reduce the net energy barrier, causing an increase in the overall diffusivity. This tendency is reversed as the CH_4 loading become very high and steric hindrance effects reduce the possibility of CH_4 molecules hopping from cage to cage. This behavior has been seen in the diffusion in a variety of nanoporous materials with cages separated by sizable energy barriers.[9,28,36,38−42]

Unlike CH_4, the diffusivity of CO_2 decreases monotonically as the loading is increased. This occurs because adsorbed CO_2 molecules preferentially occupy the 8MR windows and, while in these positions, block hopping by other CO_2 molecules. The fact that the preferred site for CO_2 can accommodate only one molecule makes this situation quite different from the behavior of CH_4, where multiple molecules can coexist in the preferred adsorption sites.

In measuring CH_4 diffusion in DDR, we used TST-based KMC methods because MD cannot measure slow diffusion in the range of 10^{-8} cm^2/s, as discussed above. One outcome from our calculations is that for a small range of CH_4 loadings, the diffusivities predicted via this TST-based KMC method are larger than 10^{-7} cm^2/s. We therefore performed MD simulations to examine CH_4 diffusion at these loadings (14−18 molecules/unit cell). The results from these MD calculations are shown in Figure 8. The close agreement between these MD results and our TST-based KMC calculations provides strong support for the validity of the latter approach.

6. Mixture Diffusion of CO_2 and CH_4

We now turn to the diffusion of CH_4/CO_2 mixtures in DDR. For the same reasons discussed before, it is not possible to directly characterize diffusion of both species using MD. We therefore used an approach in which CO_2 diffusion as part of an adsorbed mixture was directly characterized using MD, while CH_4 diffusion as part of a mixture was described using an extension of our TST-based KMC approach that includes rapidly diffusing CO_2 molecules. Results from each of these calculations are discussed below.

Because of the relatively rapid diffusion of CO_2 in adsorbed mixtures, we used MD simulations to describe CO_2 self-diffusion in CO_2/CH_4 mixtures. For MD simulations of this kind, the system was initialized by $(2 \times 10^7)-(4 \times 10^7)$ GCMC steps to get an appropriate distribution of the adsorbed molecules,

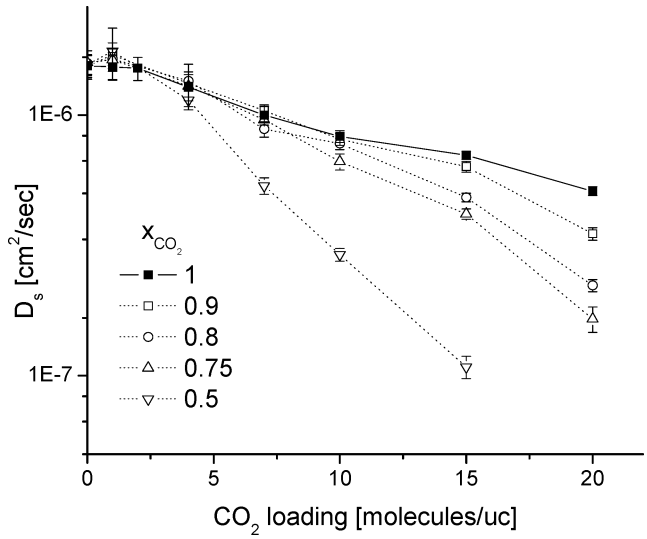

Figure 10. Self-diffusivities of CO_2 in CO_2/CH_4 mixtures as a function of CO_2 loading at various compositions with single-component diffusion of CO_2.

followed by 1.5×10^7 canonical MC moves and 1.5×10^7 steps of MD for equilibration. Subsequently, MD data were collected for 20 ns with a 1 fs time step. At each loading, five independent trajectories were used to measure the self-diffusion of CO_2. Because CO_2 adsorbs preferentially relative to CH_4 in DDR, we only examined adsorbed loadings with CO_2 mole fractions varying from 0.9 to 0.5. At a pressure of 2 (20) bar, for example, a bulk phase composition that is 10% CO_2 and 90% CH_4 is in equilibrium with an adsorbed phase that is 43.8% (48.3%) CO_2 (cf., Figure 5).

The CO_2 self-diffusivities observed in these MD simulations are shown in Figure 10. The most important observation from these results is that the diffusion of CO_2 is not greatly affected by CH_4 at most physically relevant mixture compositions. For loadings of 10 CO_2 molecules/unit cell or less, the CO_2 diffusivity is only reduced significantly when the adsorbed phase is 50% CH_4, a situation that requires a gas phase with >90% CH_4. This is a very unusual result; it is typical in the diffusive transport of gas mixtures to find that the diffusivity of the more mobile species is reduced by the presence of a slower species.[15,18,20] This unusual (and potentially useful) outcome occurs because of the different adsorption sites and diffusion mechanisms of the two species.

To include CO_2 in our TST-based KMC simulation of CH_4 diffusion, we assumed that CO_2 can be treated as being at equilibrium in our lattice model because CO_2 diffuses much more quickly than CH_4. This assumption was strongly supported by direct examination of MD trajectories from adsorbed mixtures. We therefore treated the population of CO_2 in the 8MR windows using the solid curve shown in Figure 7 for all adsorbed mixtures. When a CO_2 molecule was present in an 8MR, the hopping rate for CH_4 through that window was assumed to be zero. At every step in our KMC simulation, the population of each 8MR window was assigned randomly.

We also assumed that the quantities appearing in the integrals in eq 1 were only dependent on the molecules in the cages. This means that the TST-based calculations we discussed above can be extended to describe CH_4 hopping rates as a function of the number of CH_4 and CO_2 molecules in each cage. We applied the histogram methods defined previously to calculate the hopping rate of CH_4 molecules from cage i to cage j in terms

(36) Beerdsen, E.; Dubbeldam, D.; Smit, B. *Phys. Rev. Lett.* **2006**, *96*, 044501.
(37) Selassie, D.; Davis, D.; Dahlin, J.; Feise, E.; Haman, G.; Sholl, D. S.; Kohen, D. *J. Phys. Chem. C* **2008**, *112*, 16521–16531.
(38) Skoulidas, A. I.; Sholl, D. S. *J. Phys. Chem. B* **2005**, *109*, 15760–15768.
(39) Skoulidas, A. I.; Sholl, D. S. *J. Phys. Chem. A* **2003**, *107*, 10132–10141.
(40) Krishna, R.; van Baten, J. M. *Microporous Mesoporous Mater.* **2008**, *109*, 91–108.
(41) Krishna, R.; van Baten, J. M. *Chem. Eng. Sci.* **2008**, *63*, 3120–3140.
(42) Beerdsen, E.; Smit, B.; Dubbeldam, D. *Phys. Rev. Lett.* **2004**, *93*, 248301.

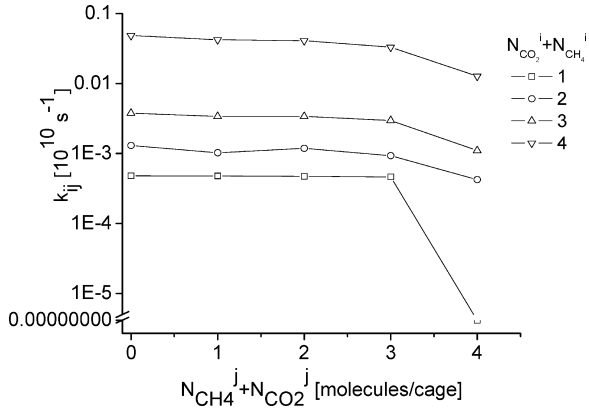

Figure 11. Similar to Figure 9, but for hopping of CH_4 in adsorbed CH_4/CO_2 mixtures. The horizontal axis and legend show the total number of molecules in the final cage and initial cage for the hopping CH_4 molecule, respectively.

of the numbers of molecules in each cage, $k_{ij} = k_{ij}(n_{CH_4,i},n_{CH_4,j},n_{CO_2,i},n_{CO_2,j})$. Calculations of this kind were performed for 0−4 CO_2 molecules per cage and 0−2 CH_4 molecules, a range that allows us to describe almost all possible adsorbed loadings. For each rate calculation, 10^8 canonical MC moves per particle were used to equilibrate the system, and 2×10^8 canonical moves per particle were used to produce data. The hopping rates for CH_4 calculated using this approach are shown in Figure 11.

Using our TST-based KMC model, we examined CH_4 self-diffusion at a range of mixture loadings. At each loading, the system was equilibrated for $>1.5 \times 10^5$ KMC steps per particle, and data were produced from 5×10^5 steps per particle. Figure 12 shows the calculated CH_4 diffusivities in adsorbed CH_4/CO_2 mixtures. The response of CH_4 to CO_2 is quite different from the effect of CH_4 on CO_2 because the presence of adsorbed CO_2 reduces the diffusivity of CH_4. At low loadings, the diffusivity of CH_4 in mixtures is reduced to ∼40−80% of the values for single-component CH_4, and larger decreases are seen at higher loadings.

It is useful to discuss the diffusion of CH_4 in the presence of adsorbed CO_2 in terms of two competing effects. First, the presence of adsorbed CO_2 tends to block the 8MR windows in DDR and hinders CH_4 diffusion. The diffusivity obtained from a KMC simulation that included these effects but no other CO_2 effect is shown in Figure 12b. As expected, this effect reduces the diffusivity of CH_4 at all loadings. The presence of CO_2 also has an effect on the cage-to-cage hopping rates for CH_4 molecules. Similar to what is seen for single-component adsorbed CH_4, the presence of CO_2 molecules in cages acts to reduce the net energy barrier for hopping of CH_4 molecules. This effect is quantified in Figure 12b by results from a KMC simulation that included the effects of CO_2 in our TST-based rate calculations but did not include window blocking effects. It is evident from this figure that this effect increases the diffusivity of CH_4. The overall influence of CO_2 on the diffusion of CH_4 occurs through a combination of these two effects, leading to the net outcome shown in Figure 12a.

A useful way to further illustrate the unusual properties of molecular diffusion in DDR is to compare our observations with the results of a correlation that have been developed to predict mixture properties from single-component data. A particularly successful correlation for the self-diffusion of molecular mixtures in zeolites and other nanopores was introduced by Krishna

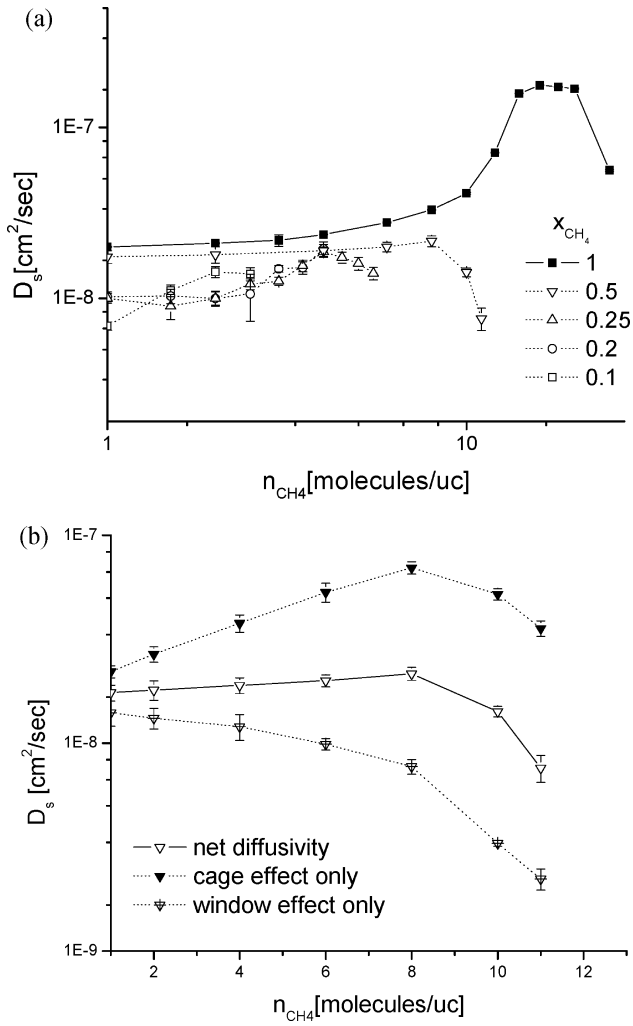

Figure 12. CH_4 diffusion data from CH_4/CO_2 mixtures in DDR, showing (a) self-diffusivities of CH_4 loading at various mixture compositions, and (b) the self-diffusion of CH_4 in an equimolar adsorbed mixture ($x_{CH_4=0.5}$), showing the separate effects from cage occupation by CO_2 and window blocking by CO_2.

and Paschek.[15] In the mixture, two diffusion coefficients can define the correlation effects, the self-exchange coefficient, D^{ii}_{corr}, and binary-exchange coefficient, D^{ij}_{corr}. Once the single-component self- and corrected diffusivities are known, the self-exchange coefficients are defined via

$$D^i_s(\theta) = \frac{1}{\dfrac{1}{D^i_o(\theta)} + \dfrac{\theta_i}{D^{ii}_{corr}}} \tag{3}$$

Here, θ_i is fractional loading of species i in binary mixture with species j. $D_s{}^i$ is the self-diffusivity, and $D_o{}^i$ is the pure component corrected diffusivity of species i. The binary-exchange coefficients, D^{ij}_{corr}, reflecting correlation effects between different species in a mixture, are then estimated using

$$q^j_{sat}D^{ij}_{corr}(\theta) = [q^j_{sat}D^{ii}_{corr}(\theta)]^{\theta_i/(\theta_i+\theta_j)}[q^i_{sat}D^{jj}_{corr}(\theta)]^{\theta_j/(\theta_i+\theta_j)} \tag{4}$$

Here, $q_{sat}{}^i$ is saturation loading for species i. Finally, the binary self-diffusivities in the mixture are predicted using

$$D^i_s = \frac{1}{\dfrac{1}{D^i_o} + \dfrac{\theta_i}{D^{ii}_{corr}} + \dfrac{\theta_j}{D^{ij}_{corr}}} \tag{5}$$

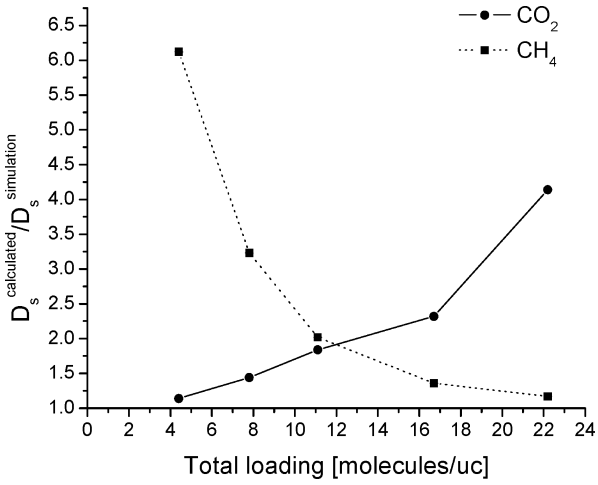

Figure 13. The ratio of the predicted mixture self-diffusivities from Krishna and Paschek's formulation to the simulation data from our work at $x_{CO_2=0.9}$ as a function of total loading. "●" and "■" denote CO_2 and CH_4 data.

This correlation has given relatively good predictions in a variety of nanoporous materials, including the silica zeolites ITQ-7, FAU, AFI, and MFI,[15,18,37,40,41,43] carbon nanotubes,[16] and CuBTC.[44] Using the earlier force-field for CO_2 and CH_4 in DDR, Krishna et al. showed this correlation did not accurately capture the mixture diffusivities seen in mixture MD simulations in DDR.[9,10] Because our new force-field predicts molecular diffusion coefficients that are considerably slower than those from the earlier MD calculations (in accord with experimental observation, as discussed above), it is useful to revisit the ability of Krishna and Paschek's correlation for describing CO_2/CH_4 mixture diffusion in DDR.

The accuracy of Krishna and Paschek's correlation for describing CH_4/CO_2 mixtures at $x_{CO_2} = 0.9$ in DDR is shown in Figure 13. The ratios of the predicted diffusivities over calculated ones were represented as a function of total loading with error bars. For both species, the ratio is far from 1, indicating deviation of the predicted values from simulation data. The deviation was particularly large at higher total loadings for CO_2 and at lower total loadings for CH_4. Similar tendencies were observed at all other compositions we examined (data not shown). In light of the diffusion mechanisms that exist in DDR, it is not surprising that this correlation gives inaccurate results, because the correlation is based on the heuristic idea that the adsorbing molecules are well mixed.

7. Conclusion

The development of materials that can efficiently separate CO_2 from other gases has the potential to allow large-scale mitigation of CO_2 emissions. The efficient separation of CO_2 and CH_4 is challenging because of the similar size of these two molecules. This specific separation has great practical significance because of the large volumes of CO_2-contaminated natural gas that are known worldwide. We have shown that the diffusion mechanisms of CO_2 and CH_4 in the silica zeolite DDR have unusual and potentially useful properties that make this material attractive as a membrane for CO_2/CH_4 separations.

Our results required several methodological advances that were crucial for an accurate description of DDR and will also be relevant for modeling of other small pore zeolites. We have introduced new force-fields to simulate these adsorbed species that for the first time correctly capture the experimentally observed adsorption and dilute loading diffusion data. Previous molecular simulations of DDR used force-fields that greatly overpredicted the diffusion rates of both molecular species, so they could not give reliable information on the performance of DDR as a membrane. Once the diffusion of CH_4 is described accurately in DDR, it is clear that MD is not suitable for characterizing this slowly diffusing species. We introduced a transition state theory-based approach that rigorously describes the loading-dependent diffusion of CH_4, both as a single adsorbed component and when it is adsorbed as a part of a mixture with the more rapidly diffusing CO_2. All of our calculations have been reported for adsorbed mixtures at room temperature. For a number of applications involving CO_2/CH_4 separations, it would be desirable to treat gas mixtures at higher temperatures, 100 °C, for example. The strong separation in time scales between the hopping of CH_4 and CO_2 molecules in DDR at room temperature would also persist at these elevated temperatures, so the observations we have made about the mechanisms of mixture diffusion in DDR and the methods we have introduced here will also be applicable at these elevated temperatures.

It is well-known that CO_2 adsorbs preferentially in DDR relative to CH_4. The typical expectation in nanoporous materials is that the more strongly adsorbing species will diffuse more slowly than the more weakly adsorbing species. Moreover, diffusion in mixtures is expected to occur via what can be thought of reversion to the mean; the existence of a slowly diffusing species slows down more rapidly diffusing molecules and vice versa. These expectations mean that, in general, a nanoporous membrane will have lower selectivity than when the same material is used in an adsorption-based separation, and the selectivity of a membrane for a permeating mixture will be less pronounced than the selectivity that would be predicted from single-component experiments. The key macroscopic observation from our calculations is these expectations are incorrect for CO_2/CH_4 diffusion in DDR. As was already known from experiments, single-component CO_2 diffuses much more rapidly than does CH_4 at dilute loadings. Our detailed calculations predict that in adsorbed mixtures of CO_2 and CH_4, the rapidly diffusing CO_2 is only slightly affected by the presence of CH_4, while the slowly diffusing CH_4 is strongly retarded by the presence of CO_2. This situation is very unusual, and it occurs because the two molecules prefer different kinds of adsorption sites inside DDR. CO_2 molecules prefer to sit in the 8MR windows that separate DDR's cages, but these same windows are the transition states for hopping of CH_4 molecules from cage to cage. This prediction has the important practical implication that membranes made from DDR can be expected to have a significantly higher performance for CO_2/CH_4 separations than would be predicted on the basis of adsorption data alone. It seems likely that this situation is not unique to DDR, so our methods should make it possible to search for other small pore zeolites with similarly attractive properties.

Acknowledgment. This work was funded by the NSF through grant CBET0553861 and through funding from ExxonMobil. Helpful conversations with H. Chen, N. Corcoran, H. Deckman, and D. Ruthven are gratefully acknowledged.

JA901483E

(43) Skoulidas, A. I.; Sholl, D. S.; Krishna, R. *Langmuir* **2003**, *19*, 7977–7988.
(44) Keskin, S.; Liu, J.; Johnson, K.; Sholl, D. S. *Langmuir* **2008**, *24*, 8254–8261.